PoS -(LAT2009-) 145; 2009
DESY 09-176

PROCEEDINGS OF SCIENCE

Nucleon form factors with $N_F = 2$ twisted mass fermions

C. Alexandrou[*] [(a,b)], **T. Korzec**[†][(a)], **G. Koutsou** [(a,c)]

[(a)] *Department of Physics, University of Cyprus, P.O. Box 20537, 1678 Nicosia, Cyprus*
[(b)] *Computation-based Science and Technology Research Center, Cyprus Institute, 15 Kypranoros St., 1645 Nicosia, Cyprus*
[(c)] *Bergische Universität Wuppertal, Fachbereich Physik, 42097 Wuppertal, Germany and JSC and IAS, FZ Jülich, 52425 Jülich, Germany*
E-mail: alexand@ucy.ac.cy, korzec@ucy.ac.cy, i.koutsou@fz-juelich.de

R. Baron, P. Guichon
CEA-Saclay, IRFU/Service de Physique Nucléaire, 91191 Gif-sur-Yvette, France
E-mail: remi.baron@cea.fr, pierre.guichon@cea.fr

M. Brinet, J. Carbonell, P.-A. Harraud
Laboratoire de Physique Subatomique et Cosmologie, UJF/CNRS/IN2P3, 53 avenue des Martyrs, 38026 Grenoble, France
E-mail: mariane@lpsc.in2p3.fr, Jaume.Carbonell@lpsc.in2p3.fr, harraud@lpsc.in2p3.fr

K. Jansen,
NIC, DESY, Platanenallee 6, D-15738 Zeuthen, Germany
Email: Karl.Jansen@desy.de

arXiv:0910.3309v2 [hep-lat] 22 Oct 2009

We present results on the electromagnetic and axial nucleon form factors using two degenerate flavors of twisted mass fermions on lattices of spatial size 2.1 fm and 2.7 fm and a lattice spacing of about 0.09 fm. We consider pion masses in the range of 260-470 MeV. We chirally extrapolate results on the nucleon axial charge, the isovector Dirac and Pauli root mean squared radii and magnetic moment to the physical point and compare to experiment.

The XXVII International Symposium on Lattice Field Theory - LAT2009
July 26-31 2009
Peking University, Beijing, China

[*] Speaker.
[†] Current address:Institut für Physik Humboldt Universität zu Berlin, Newtonstrasse 15, 12489 Berlin, Germany.

© Copyright owned by the author(s) under the terms of the Creative Commons Attribution-NonCommercial-ShareAlike Licence.

1. Introduction

Twisted mass fermions [1] provide an attractive formulation of lattice QCD that allows for automatic $\mathcal{O}(a)$ improvement, infrared regularization of small eigenvalues and fast dynamical simulations. A particularly attractive feature for the calculation of the nucleon form factors discussed in this work is the automatic $\mathcal{O}(a)$ improvement obtained by tuning only one parameter, requiring no further improvements on the operator level. Important physical results are emerging using gauge configurations generated with two degenerate flavors of twisted quarks ($N_F = 2$) in both the meson [2] and baryon [3] sectors. An example is the accurate determination, using precise results in the meson sector, of low energy constants of great relevance to phenomenology. Currently, $N_F = 2$ simulations are available for pion mass in the range of about 260-470 MeV for three lattice spacings $a < 0.1$ fm allowing for continuum and chiral extrapolations. In this work we discuss high-statistics results on the nucleon form factors obtained at one value of the lattice spacing. Electromagnetic and axial form factors (FFs) of the proton and the neutron are fundamental quantities that yield information on their internal structure such as their size, magnetization and axial charge. They have been studied experimentally for a long time improving their measuements both in terms of precision as well as in terms of probing larger momentum transfers. Several lattice collaborations are currently using dynamical fermions to calculate these fundamental quantities [4, 5].

The action for two degenerate flavors of quarks in twisted mass QCD is given by

$$S = S_g + a^4 \sum_x \bar{\chi}(x) \left[\frac{1}{2}\gamma_\mu(\nabla_\mu + \nabla^*_\mu) - \frac{ar}{2}\nabla_\mu\nabla^*_\mu + m_{\rm crit} + i\gamma_5\tau^3\mu \right] \chi(x) \quad , \tag{1.1}$$

where we use the tree-level Symanzik improved gauge action S_g. The quark fields χ are in the so-called "twisted basis" obtained from the "physical basis" at maximal twist by the transformation $\psi = \frac{1}{\sqrt{2}}[\mathbf{1} + i\tau^3\gamma_5]\chi$ and $\bar{\psi} = \bar{\chi}\frac{1}{\sqrt{2}}[\mathbf{1} + i\tau^3\gamma_5]$. We note that, in the continuum, this action is equivalent to QCD. A crucial advantage is the fact that by tuning a single parameter, namely the bare untwisted quark mass to its critical value $m_{\rm cr}$, physical observables are automatically $\mathcal{O}(a)$ improved. A disadvantage is the explicit flavor symmetry breaking. In a recent paper we have checked that this breaking is small for baryon observables for the lattice spacing discussed here [6].

To extract the nucleon FFs we need to evaluate the nucleon matrix elements $\langle N(p_f, s_f)|j_\mu|N(p_i, s_i)\rangle$, where $|N(p_f, s_f)\rangle$, $|N(p_i, s_i)\rangle$ are nucleon states with final (initial) momentum $p_f(p_i)$ and spin $s_f(s_i)$ and j_μ is either the electromagnetic current $V^{EM}_\mu(x) = \frac{2}{3}\bar{u}(x)\gamma_\mu u(x) - \frac{1}{3}\bar{d}(x)\gamma_\mu d(x)$ or the axial current $A^a_\mu(x) = \bar{\psi}(x)\gamma_\mu\gamma_5\frac{\tau^a}{2}\psi(x)$. Whereas the matrix element of the axial current receives contributions only from the connected diagram shown in Fig. 1 the electromagnetic one has, in addition, disconnected contributions. In the isospin limit the matrix element of the isovector electromagnetic current $V^a_\mu(x) = \bar{\psi}(x)\gamma_\mu\frac{\tau^a}{2}\psi(x)$ has no disconnected contributions [7]. Therefore in this work we only evaluate the isovector nucleon FFs obtained from the connected diagram.

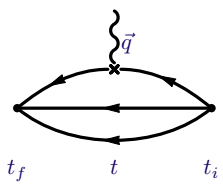

Fig.1: Connected nucleon three-point function.

The electromagnetic matrix element of the nucleon can be expressed in terms of the Dirac and Pauli form factors, F_1 and F_2 defined, in Euclidean time, as

$$\langle N(p_f,s_f)|V_\mu(0)|N(p_i,s_i)\rangle = \sqrt{\frac{m_N^2}{E_N(\vec{p}_f)E_N(\vec{p}_i)}}\overline{u}(p_f,s_f)\mathscr{O}_\mu u(p_i,s_i),\ \mathscr{O}_\mu = \gamma_\mu F_1(Q^2)+\frac{i\sigma_{\mu\nu}q^\nu}{2m_N}F_2(Q^2)$$

with $q = p_f - p_i$ the momentum transfer and $Q^2 = -q^2$. These are related to the Sachs electric G_E and magnetic G_M FFs via: $G_E(Q^2) = F_1(Q^2) - \frac{Q^2}{(2m_N)^2}F_2(Q^2)$ and $G_M(Q^2) = F_1(Q^2) + F_2(Q^2)$.

Similarly, the axial current matrix element of the nucleon $\langle N(p_f,s_f)|A^a_\mu(0)|N(p_i,s_i)\rangle$ can be expressed in terms of the form factors G_A and G_p with $\mathscr{O}_\mu$ given by

$$\mathscr{O}_\mu = \left[-\gamma_\mu\gamma_5 G_A(Q^2) + i\frac{q^\mu\gamma_5}{2m_N}G_p(Q^2)\right]\frac{\tau^a}{2}.$$

2. Lattice evaluation

The nucleon interpolating field in the physical basis $J(x) = \varepsilon^{abc}\left[u^{a\top}(x)\mathscr{C}\gamma_5 d^b(x)\right]u^c(x)$ can be written in the twisted basis at maximal twist as $\tilde{J}(x) = \frac{1}{\sqrt{2}}[\mathbb{1}+i\gamma_5]\varepsilon^{abc}\left[\tilde{u}^{a\top}(x)\mathscr{C}\gamma_5\tilde{d}^b(x)\right]\tilde{u}^c(x)$. The transformation of the electromagnetic current, $V^a_\mu(x)$, to the twisted basis leaves the form of $V^{0,3}_\mu(x)$ unchanged. We use the Noether lattice current and therefore the renormalization constant $Z_V = 1$. The axial current A^3_μ also has the same form in the two bases. In this case we use the local current and therefore we need the renormalization constant Z_A. The value of $Z_A = 0.76(1)$ [8] was determined non-perturbatively in the RI'-MOM scheme. This value is consistent with a recent analysis [9], which uses a perturbative subtraction of $\mathscr{O}(a^2)$ terms [10] for a better identification of the plateau yielding a value of $Z_A = 0.768(3)$ [9]. In order to increase overlap with the proton state and decrease overlap with excited states we use Gaussian smeared quark fields [11] for the construction of the interpolating fields: $\mathbf{q}^a(t,\vec{x}) = \sum_{\vec{y}} F^{ab}(\vec{x},\vec{y};U(t))\ q^b(t,\vec{y})$ with $F = (\mathbb{1}+\alpha H)^n$ and $H(\vec{x},\vec{y};U(t)) = \sum_{i=1}^3[U_i(x)\delta_{x,y-\hat{\imath}} + U_i^\dagger(x-\hat{\imath})\delta_{x,y+\hat{\imath}}]$. In addition we apply APE-smearing to the gauge fields U_μ entering H. The smearing is the same as for our calculation of baryon masses with the smearing parameters α and n optimized for the nucleon ground state [3].

To set the scale we use the nucleon mass in the physical limit. We show in Fig. 2 results at three values of the lattice spacings corresponding to $\beta = 3.9$, $\beta = 4.05$ and $\beta = 4.2$. As can be seen, cut-off effects are negligible and we can therefore use continuum chiral perturbation theory to extrapolate to the physical point. We correct for volume dependence coming from pions propagating around the lattice [12]. To chirally extrapolate we use the well-established $\mathscr{O}(p^3)$ result of heavy baryon chiral perturbation theory (HBχPT) given by

$$m_N = m_N^0 - 4c_1m_\pi^2 - \frac{3g_A^2}{16\pi f_\pi^2}m_\pi^3. \tag{2.1}$$

We perform a fit to the volume corrected results at $\beta = 3.9$, $\beta = 4.05$ and $\beta = 4.2$ and extract $r_0 = 0.462(5)$ fm. Fitting instead to the $\beta = 3.9$, $\beta = 4.05$ results we find $r_0 = 0.465(6)$ fm showing that indeed cut-off effects are small. To estimate the error due to the chiral extrapolation we use HBχPT to $\mathscr{O}(p^4)$, which leads to $r_0 = 0.489(11)$. We take the difference between the $\mathscr{O}(p^3)$ and $\mathscr{O}(p^4)$ mean values as an estimate of the uncertainty due to the chiral extrapolation. Fits to other higher order χPT formulae shown in Fig.3 and described in Ref. [3] are consistent with $\mathscr{O}(p^4)$ HBχPT. Using $r_0 = 0.462(5)(27)$ and the computed r_0/a ratios we obtain $a_{\beta=3.9} = 0.089(1)(5)$,

$a_{\beta=4.05} = 0.070(1)(4)$ and $a_{\beta=4.2} = 0.056(2)(3)$. These values are consistent with the lattice spacings determined from f_π and will be used for converting to physical units in what follows. We note that results on the nucleon mass using twisted mass fermions agree with those obtained using other lattice $\mathcal{O}(a^2)$ formulations for lattice spacings below 0.1 fm [6].

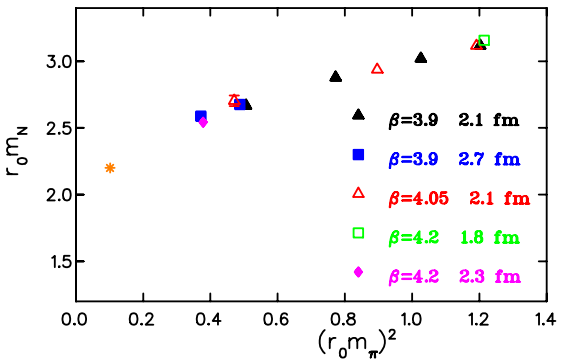

Fig.2: Nucleon mass in units of r_0 at 3 lattice spacings and spatial lattice size L such that $m_\pi L > 3.5$.

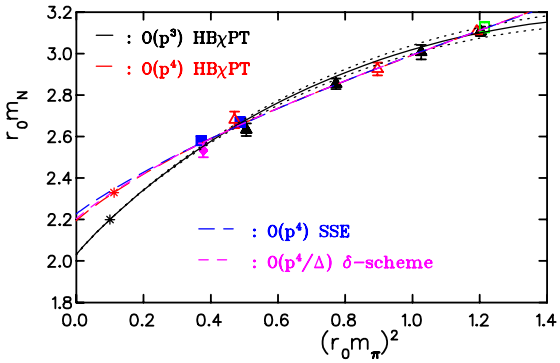

Fig.3: Nucleon mass in units r_0. The solid and dashed lines are fits to $\mathcal{O}(p^3)$ and $\mathcal{O}(p^4)$ HBχPT.

In order to calculate the aforementioned nucleon matrix elements we calculate respectively the two-point and three-point functions: $G(\vec{q},t_f) = \sum_{\vec{x}_f} e^{-i\vec{x}_f\cdot\vec{q}}\,\Gamma^0_{\beta\alpha}\,\langle J_\alpha(t_f,\vec{x}_f)\overline{J}_\beta(0)\rangle$ and $G^\mu(\Gamma^\nu,\vec{q},t) = \sum_{\vec{x},\vec{x}_f} e^{i\vec{x}\cdot\vec{q}}\,\Gamma^\nu_{\beta\alpha}\,\langle J_\alpha(t_f,\vec{x}_f)\,j^\mu(t,\vec{x})\overline{J}_\beta(0)\rangle$, where the projection matrices $\Gamma^0 = \frac{1}{4}(\mathbb{1}+\gamma_0)$ and $\Gamma^k = i\Gamma^0\gamma_5\gamma_k$. The kinematical setup that we used is illustrated in Fig. 1: We create the nucleon at $t_i = 0$, $\vec{x} = 0$ (source) and annihilate it at $t_f/a = 12$, $\vec{p}_f = 0$ (sink). We checked that the sink-source time separation of $12a$ is sufficient for the isolation of the nucleon ground state by comparing the results with those obtained when $t_f/a = 14$ is used [7]. We insert the current j^μ at t carrying momentum $\vec{q} = -\vec{p}_i$. In this work we limit ourselves to the calculation of the connected diagram which in the isospin limit yields the isovector electromagnetic form factors. This is calculated by performing sequential inversions through the sink so that no new inversions are needed for different operator $j^\mu(t,\vec{q})$. However new inversions are necessary for a different choice of the projection matrices Γ^α. In this work, we consider the four choices given above, which are optimal for the form factors considered here and construct the ratio

$$R^\mu = \frac{G^\mu(\Gamma,\vec{q},t)}{G(\vec{0},t_f)}\sqrt{\frac{G(\vec{p}_i,t_f-t)G(\vec{0},t)G(\vec{0},t_f)}{G(\vec{0},t_f-t)G(\vec{p}_i,t)G(\vec{p}_i,t_f)}} \overset{t_f-t,t\to\infty}{\longrightarrow} \Pi^\mu(\Gamma,\vec{q}) \quad . \tag{2.2}$$

The leading time dependence and overlap factors cancel yielding as the plateau value $\Pi^\mu(\Gamma,\vec{q})$ from which we extract the form factors using the relations

$$\Pi^\mu(\Gamma^0,\vec{q}) = \frac{c}{2m}[(m+E)\delta_{0,\mu} + iq_k\delta_{k,\mu}]\;G_E(Q^2), \quad \Pi^i(\Gamma^k,\vec{q}) = \frac{c}{2m}\sum_{jl}\varepsilon_{jkl}q_j\delta_{l,i}\,G_M(Q^2)$$

and $\Pi^{5i}(\Gamma^k,\vec{q}) = \frac{ic}{4m}\left[\frac{q_kq_i}{2m}\,G_p(Q^2) - (E+m)\delta_{i,k}\,G_A(Q^2)\right], \quad k=1,\cdots,3,$ where $c = \sqrt{\frac{2m^2}{E(E+m)}}$.

3. Results

3.1 Isovector electromagnetic form factors

The isovector electric and magnetic form factors at $\beta = 3.9$ are shown in Figs. 4 and 5 respec-

tively on lattices of size $24^3 \times 48$ and $32^3 \times 64$ and for the pion masses and statistics listed in Fig. 6.

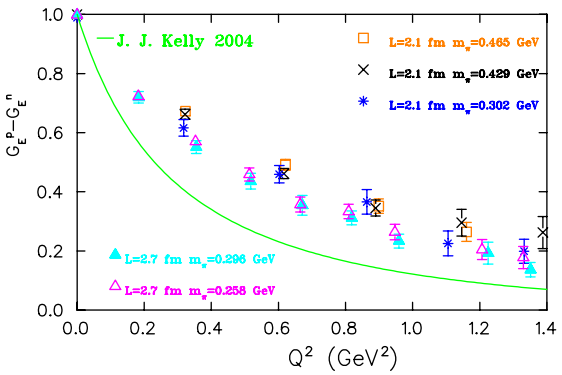

Fig. 4: The isovector electric form factor as a function of Q^2 compared to experiment (solid curve).

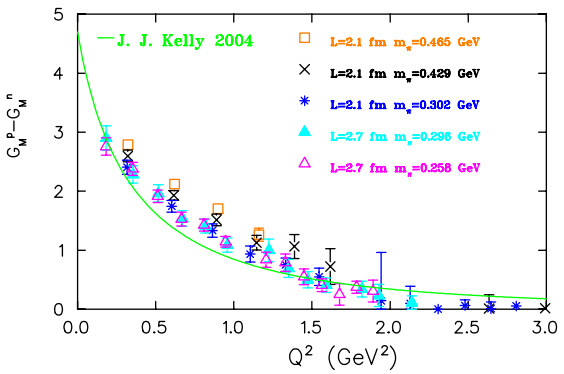

Fig. 5:The isovector magnetic form factor as a function of Q^2 compared to experiment (solid curve).

By fitting the isovector magnetic form factor to a dipole form we extract the isovector magnetic moment and Dirac and Pauli root mean squared (r.m.s.) radii shown in Figs. 6 and 7. As can be seen, the results obtained using twisted mass fermions are in agreement with recent results using dynamical domain wall fermions (DWF). Heavy baryon chiral perturbation theory to one-loop [13] can be used to extrapolate to the physical point. In the case of the Dirac r.m.s radius we fit the product $r_2^2\kappa_v$ so that only one fit parameter enters just as in the case of r_1^2. This shifts the curve but does not affect its slope. We show fits to our results alone as well as when we include the results obtained by the RBC-UKQCD collaborations [4]. The magnetic moment with three fit parameters is reproduced whereas for r_1^2 we obtained a weaker dependence on the pion mass as compared to the one predicted in chiral expansions.

m_π (GeV)	no. of confs	L
0.258	667	32
0.296	231	32
0.302	944	24
0.373	210	24
0.429	365	24
0.465	477	24

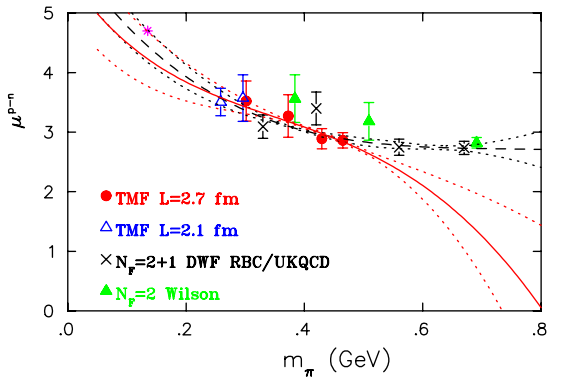

Fig. 6: The anomalous isovector magnetic moment of the nucleon.

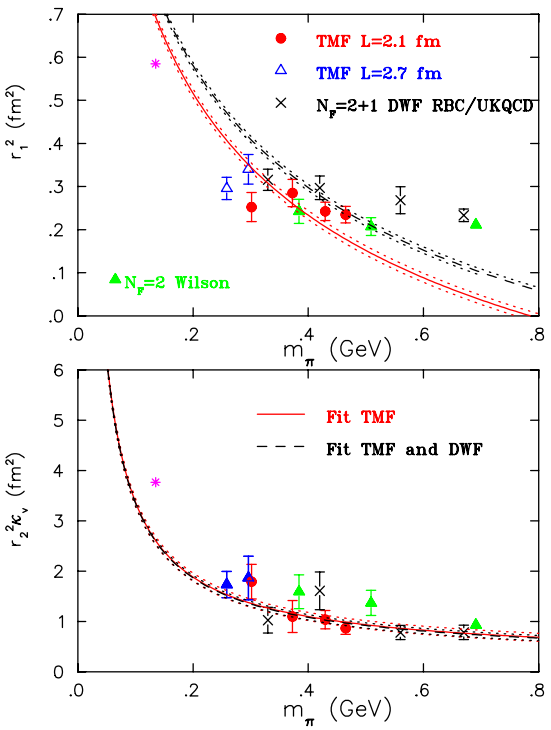

Fig 7: The Dirac (upper) and Pauli (lower) r.m.s radii.

3.2 Axial charge

Our results on the nucleon axial charge are shown in Fig. 8 and are in agreement with those obtained using domain wall fermions. Within our errors no sizable finite volume effects are observed. In order to extrapolate to the physical point we use one-loop chiral perturbation theory in the small scale expansion [14].

There are three parameters to fit: $g_A(0)$, the value of the axial charge at the chiral point, g_1 and a counter-term C_{SSE}. Fitting using the TMF results we find $g_A(0) = 1.10(13)$, $g_1 = 6.05(4.66)$ and $C_{SSE} = -3.65(3.58)$. The parameters g_1 and C_{SSE} are highly correlated explaining the resulting large error band. Including in the fit the DWF data that span larger pion masses we obtain a very different curve, showing the sensitivity in the chiral extrapolation of g_A.

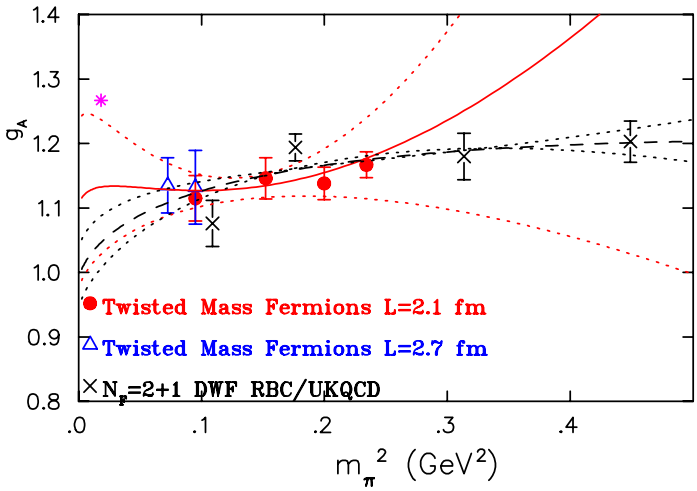

Fig. 8: The nucleon axial charge. The solid (dashed) curve is a chiral fit using TMF (TMF and DWF) results.

3.3 Axial form factors

Results for the axial form factors $G_A(Q^2)$ and $G_p(Q^2)$ are shown in Figs. 9 and 10 respectively. We perform a dipole fit to $G_A(Q^2)$ extracting an axial mass larger than in experiment as expected from the smaller slope shown by the lattice data both for TMF and DWF. Assuming pion pole dominance we can relate the form factor $G_p(q^2)$ to $G_A(Q^2)$. Using the pion mass measured on the lattice we predict the dashed curve shown in Fig. 10. Our lattice data on $G_p(q^2)$ are flatter than pion pole dominance predicts requiring a larger pole mass than the pion mass. Large volume effects are expected at low Q^2 indicated by the deviation of $G_p(Q^2)$ from the fitted curve at the smallest Q^2-value.

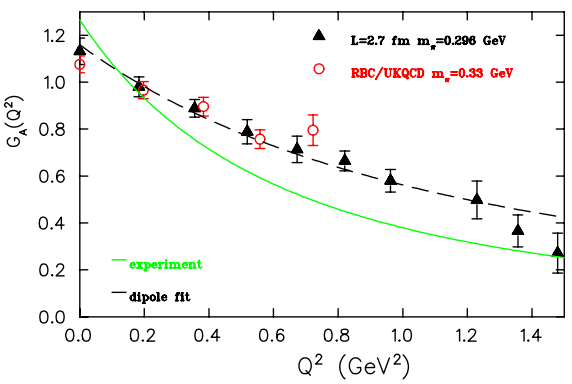

Fig. 9: Axial form factor $G_A(Q^2)$ as a function of Q^2. The dashed (solid) line is the best dipole fit to the lattice (experimental) results.

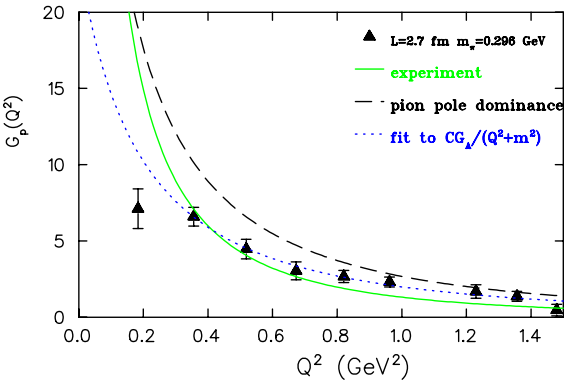

Fig. 10: The dotted line is a fit of lattice results to the form $\frac{CG_A(Q^2)}{(Q^2+m^2)}$ and the dashed (solid) line is the prediction of pion pole dominance using lattice (experimental) results on $G_A(Q^2)$.

4. Conclusions

Using $N_F = 2$ twisted mass fermions we obtain accurate results on the isovector electromagnetic G_E, G_M and axial G_A, G_p form factors as a function of Q^2 for pion mass in the range of about 260-470 MeV. The general feature is a flatter dependence on Q^2 than experiment. The Dirac r.m.s radius thus shows a weaker dependence on the pion mass than expected from chiral perturbation theory. Finite volume effects are found to be small on quantities like g_A and the isovector magnetic moment and r.m.s radii. Our results are in agreement with recent results obtained using dynamical $N_F = 2+1$ DWF. At the physical point using TMF we find $g_A = 1.13(10)$ close to the experimental value albeit with a large error due to the chiral extrapolation. An analysis of these form factors at $\beta = 4.05$ is under way so that a check of cut-off effects can be carried out.

Acknowledgments: This work was performed using HPC resources from GENCI (IDRIS and CINES) Grant 2009-052271 and was partly supported by funding received by the DFG Sonderforschungsbereich/ Transregion SFB/TR9 and the Cyprus Research Promotion Foundation under contracts EPYAN/0506/08, ΚΥ-Γ/0907/11/ and TECHNOLOGY/ΘΕΠΙΣ/0308(BE)/17.

References

[1] R. Frezzotti *et al.*, JHEP 08 (2001) 058, hep-lat/0101001.

[2] P. Boucaud *et al.*, Phys. Lett. B650 (2007) 304; K. Jansen, C. Michael and C. Urbach ([ETMC), Eur. Phys. J. C **58**, 261 (2008); B. Blossier *et al.*, JHEP **0907**, 043 (2009); K. Jansen, C. McNeile, C. Michael, C. Urbach (ETMC) arXiv:0906.4720; X. Feng, K. Jansen and D. B. Renner, arXiv:0909.3255; K. Jansen, C. Michael, A. Shindler and M. Wagner (ETMC), JHEP **0812**, 058 (2008).

[3] C. Alexandrou *et al.* (ETMC) Phys. Rev.D 78,014509 (2008), arXiv:0803.3190; C. Alexandrou, arXiv:0906.4137; C. Alexandrou *et al.* (ETMC), PoS **LAT2007**, 087 (2007); [arXiv:0710.1173]. V. Drach *et al.*, PoS **LAT2008**, 123 (2008), arXiv:0905.2894.

[4] S. Ohta and T. Yamazaki (RBC and UKQCD Collaborations), arXiv:0810.0045 [hep-lat].

[5] S. N. Syritsyn *et al.* (LHPC) arXiv:0907.4194.

[6] C. Alexandrou *et al.* (ETMC), arXiv:0910.2419.

[7] C. Alexandrou *et al.* (ETMC), arXiv:0811.0724 [hep-lat]; C. Alexandrou et al., Phys. Rev. D **74**, 034508 (2006).

[8] P. Dimopoulos et al. (ETMC) PoS **LAT2007**, 241 (2007).

[9] C. Alexandrou *et al.* (ETMC) PoS **LAT2009**, 136 (2009).

[10] M. Constantinou, H. Panagoupoulos and F. Stylianou, PoS **LAT2009**, 205 (2009); C. Alexandrou, M. Constantinou and T. Korzec, in preparation.

[11] S. Gusken, Nucl.Phys.Proc.Suppl.17, 361, (1990); C. Alexandrou, S. Gusken, F. Jegerlehner, K. Schilling, R. Sommer, Nucl.Phys. B414, 815 (1994).

[12] A. Ali Khan *et al.* (QCDSF) NPB689, 175 (2004)

[13] T. R. Hemmert and W. Weise, Eur. Phys. J. A **15**,487 (2002); M. Gockeler *et. al*, Phys. Rev. D **71**, 034508 (2005).

[14] T. R. Hemmert, M. Procura and W. Weise, Phys. Rev. D **68**, 075009 (2003).